

Realization of a semiconductor-based cavity soliton laser

Y. Tanguy, T. Ackemann,* and W. J. Firth
SUPA, Department of Physics, University of Strathclyde,
107 Rottenrow, Glasgow G4 0NG, Scotland, UK

R. Jäger
ULM Photonics GmbH, Lise-Meitner-Str. 13, 89081 Ulm, Germany

The realization of a cavity soliton laser using a vertical-cavity surface-emitting semiconductor gain structure coupled to an external cavity with a frequency-selective element is reported. All-optical control of bistable solitonic emission states representing small microlasers is demonstrated by injection of an external beam. The control scheme is phase-insensitive and hence expected to be robust for all-optical processing applications. The motility of these structures is also demonstrated.

PACS numbers: 42.55.Px, 42.65.Pc, 42.65.Tg, 42.79.Ta

Self-localized structures in driven non-equilibrium systems, loosely termed dissipative solitons, have attracted great interest because of their importance in a wide variety of fields (see e.g. [1] for a recent review). They are particularly interesting in optics – where they are usually referred to as cavity solitons (CS) – because of potential applications to the all-optical control of light, a major thrust of modern photonics (e.g. [2]). While some *laser* schemes have been proposed and/or demonstrated to sustain CS [3, 4, 5, 6, 7], no viable *cavity soliton laser (CSL)* has been developed for a major laser technology. This useful device would convert broad-area excitation into a narrow, coherent, power beam of high quality, or into a controllable number of such beams. Here we demonstrate optically-controlled excitation and erasure of tiny self-localized ‘lasers’ within a semiconductor vertical-cavity surface-emitting laser (VCSEL) structure. Our scheme is easily extensible to all types of VCSELs, and is therefore in the mainstream of laser engineering. It could have a substantial impact, both as a fundamentally-new type of laser and in the numerous technologies reliant on semiconductor lasers. Furthermore, from a fundamental point of view, the optical phase in an incoherently-pumped CS laser is an extra degree of freedom, which presents new opportunities for fundamental studies, e.g. of dynamics and interaction properties of the individual CS [8]. It will be interesting to compare the effects of phase-sensitive interactions of laser cavity solitons with the wealth of phenomena known for propagating spatial solitons [9].

The achievement, control and understanding of CS have shown remarkable progress in recent years, see, e.g., [10, 11] and Chapters 3-6 of [1]. So far, however, nearly all realized schemes have relied on driving by a broad-area holding beam of high spatial and temporal coherence. This holds in particular for semiconductor microcavities, which are ideal for photonics applications because of compactness, speed and ease of integration [11]

and where CS have been observed in a variety of configurations. Below laser threshold, these include both passive (i.e. absorbing, [12]) and active (i.e. amplifying, [11, 13]) media. Above threshold, CS have been demonstrated in lasers with injected signal [14, 15]. In all these cases, the frequency and phase of the CS is locked to that of the injected field, and so is sensitive to any phase variations or fluctuations. This enables efficient writing, erasing and manipulation of CS [16]. It also requires, however, active phase control within and between devices, and this is a drawback for applications. Hence there are advantages in removing the need for a holding beam and for phase-controlled addressing by moving to a lasing configuration with self-sustained CS. This also means that the device can draw its energy from an inexpensive, incoherent source (dc current supply in our case). Our realized *cavity soliton laser* has these important properties.

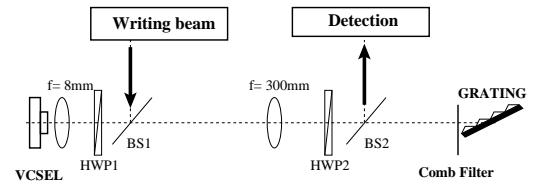


FIG. 1: Experimental apparatus. The external cavity is 616 mm long, including an 8 mm aspherical lens used as a collimator and a 300 mm lens: it is thus self-imaging, projecting a 37.5x image of the VCSEL onto a Littrow-mounted holographic diffraction grating (1800 lines/mm). Beam sampler BS1 couples a writing beam into the cavity, while BS2 couples out part of the beam for detection. Half-wave plates (HWP) are used to match the principal axes of the VCSEL, the intra-cavity beam splitters and the grating. The strong polarization dependence of the grating’s diffraction efficiency ensures that the intracavity field has a well-defined linear polarization. Hence the HWPs can be also used to control the coupling efficiency of the writing beam and of the detection arm to the external cavity. For some measurements a comb filter is added, in the re-imaged near-field close to the grating. Its slits are orthogonal to the grating lines.

*thorsten.ackemann@strath.ac.uk

either dye or photorefractive gain media [3, 4, 5] and employed intra-cavity saturable absorbers to favor bistability – a positive indicator for CS [1, 10] – between the lasing and non-lasing states. A semiconductor-based CSL would be much faster, more compact and more reliable than these systems. A recent theoretical paper considered a semiconductor CSL using a saturable absorber [7]. We adopt a different approach, based on using a VCSEL in conjunction with a frequency-selective external cavity, which is attractive as it can be implemented with essentially any VCSEL structure, using off-the-shelf optical components. Encouragingly, previous experiments have demonstrated bistability in small-area VCSELs in similar feedback configurations [17, 18]. The mechanism for bistability was shown to be due to phase-amplitude coupling [19], by which the different carrier densities of the lasing and non-lasing states imply different refractive index, and hence different cavity resonance frequencies. There can thus be a stable non-lasing state, with the cavity and external (grating-controlled) frequency out of resonance, coexistent with stable in-resonance lasing [17]. Self-localization of the lasing state to form a CS sitting on a non-lasing background requires a nonlinear transverse effect to sustain “gap” states below the band of extended lasing states. Self-focusing in a broad-area VCSEL can supply such an effect. Indeed, CS have been found in a rather similar model system [20].

The experimental set-up is shown in Figure 1. The VCSEL used is a broad-area bottom-emitting device, emitting at 980 nm and electrically pumped through a 200 μm diameter circular oxide aperture. The epitaxial structure is similar to the one described in [11, 21]. The self-imaging external cavity includes two lenses and a holographic grating in Littrow configuration. Due to the self-imaging geometry, the high Fresnel number of the solitary VCSEL, and thus the potential for self-localization independent of the boundaries, is preserved. Two beam samplers are also added, one to couple out a fraction of the beam for measurements, and the other to inject a narrow writing beam (WB) from a tunable source.

The external cavity can be analyzed with the formalism of ABCDEF matrices [22], which allows for optical elements with angular dispersion. In our Littrow configuration, the angular dispersion was calculated to be 0.46 mrad/GHz, while the angular width of the VCSEL resonance is estimated from the Bragg mirror properties to be 26 mrad. Hence we estimate the bandwidth of the feedback in frequency space to be about 55 GHz.

CS are self-localized bistable structures in spatially-extended dissipative systems. This prescription is easy to check in theoretical models, but CD identification in necessarily imperfect experimental schemes is non-trivial. The established procedure (e.g. [11]) is to demonstrate (i) existence at different locations in the transverse plane of localized bistable structures with a well-defined shape and (ii) their mutual independence (e.g. by independent switch-on and switch-off). A further indicator (iii) is then ‘motility’, i.e. that they can be easily moved around by

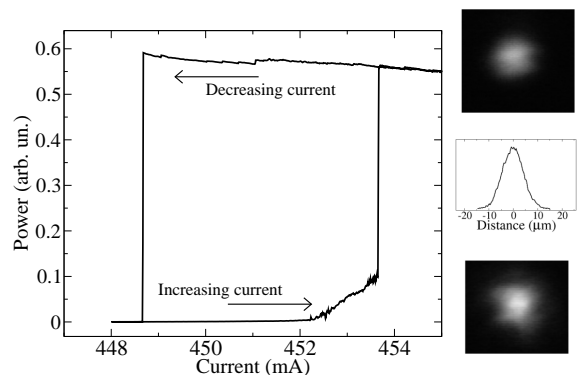


FIG. 2: Power versus current for a single spot. In this case the comb filter (explained below) was inserted in order to reduce the optical background of the spot and hence obtain a cleaner hysteresis. The panels on the right show, from top to bottom: the near-field intensity distribution around the spot, a transverse intensity profile through the center of the near-field distribution, the far-field intensity distribution.

perturbations, and hence are independent of boundary conditions and self-localized. In order to claim a CSL, the transition (iv) to narrow-band coherent emission obviously needs to be shown also.

We demonstrate fulfilment of criteria (i) and (iv) by studying the behavior of the near-field under variation of the injected current. The VCSEL is biased below the threshold of the solitary laser, and the grating is aligned so that its frequency of maximal feedback is red-detuned with respect to the longitudinal resonance frequency of the VCSEL. Increasing the injection current, we observe spontaneous formation of several localized spots, all of similar size and brightness, with a diameter of about 10 μm (FWHM; see the upper right panels in Fig. 2). These spots display bistability in dependence on current, with abrupt switch on and off (see Fig. 2, left panel). Measurements with a scanning Fabry-Perot interferometer indicate that a spot can, depending on parameters such as current and temperature, operate on one or more longitudinal modes of the external cavity (which are separated by about 240 MHz). The single-mode emission linewidth is 10 MHz, i.e., each of these spots is a tiny laser emitting coherent light.

Regarding (ii), independence and simultaneous bistability of two of these spot-lasers is demonstrated by independent switch-on and switch-off by an injected field. The sequence is shown in Fig. 3. The WB is incoherent with the spots, so that the switching is phase-insensitive. The mechanism is discussed below. We demonstrate (iii), motility of these microlasers, by perturbing them with the WB injected at some distance from the spot. They move towards it, and can be dragged around with it for significant distances (several beam diameters).

This set of observations establishes that our device is indeed a cavity soliton laser. Note that, from an applicative point of view, these experiments open up the

all-optical control of microlasers on demand.

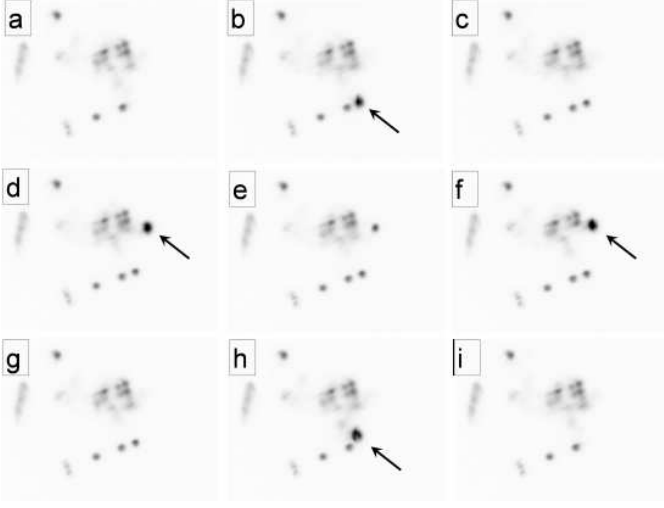


FIG. 3: Near-fields showing the successive switching on and off of two spots with an injected incoherent field (brightest spots, indicated by arrows). Dark areas correspond to high intensities. The writing beam (WB) is derived from a tunable laser source, with wavelength tuned in the vicinity of the VCSEL cavity resonance. It is focused onto the VCSEL with a $12\ \mu\text{m}$ spot diameter (FWHM) and a power in the mW range. Two sites where spontaneous spots could be observed were selected for WB injection, and the VCSEL was biased within their bistability range. a) Both spots are off, b) injection of WB, c) one spot is switched on and remains after the WB is blocked, d) injection of WB at second location, e) second spot remains on, f) WB injected beside second spot, g) second spot switched off and does not reappear (first spot unaffected), h) injection of writing beam to switch off first spot, i) both spots remain off.

Recorded spectra showed that the frequency of a specific CS could vary between successive on-switches, and could also change significantly after removal of the WB. These frequency variations can be interpreted on the basis that there is a family of CS solutions, each associated with different longitudinal modes of the external cavity. The finite frequency selectivity of the feedback allows this family to span about a 2 GHz range for a fixed current and temperature. This enables different family members to be excited by the WB, and permits noise-driven jumps between them. Thus there is no ‘memory’ of the WB frequency, which is therefore only activating CS lasing, not determining the CS properties.

Fig. 2 shows that some emission is already present (above 452 mA) before the CS actually switches on. This emission comes from low amplitude background states or patterns, visible also in Fig. 3. These are blue-detuned by some tens of GHz to the CSs and their linewidth is considerably larger. Their excitation is attributed to the finite frequency selectivity of the system. This optical background seems to be detrimental to the existence of the CSs. In order to reduce it, a comb filter was inserted in the external Littrow cavity, positioned as close

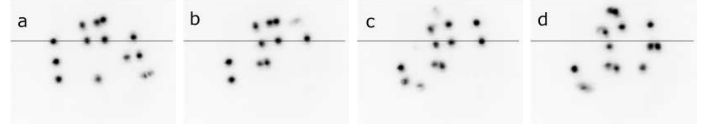


FIG. 4: Near-field displaying the effect of a comb filter placed in the external cavity at the re-imaged near-field position. Dark areas correspond to high intensities. This filter allows feedback only on several horizontal stripes with width $16\ \mu\text{m}$ at the VCSEL, spaced by the same distance. From a) to d) the comb filter is moved downwards. A line is added for reference, clearly showing that CS positions are shifted between panels. For example the rightmost CS close to the line in a) shifts quasi-continuously by about $18\ \mu\text{m}$ between a) and d). Some CSs appear and disappear spontaneously, as a result of local inhomogeneities.

as possible to the re-imaged near-field at the grating (Fig. 1). This filter allows feedback only on several horizontal stripes, and thus creates a near one-dimensional CS confinement. Figure 4 shows the resulting near-field with this filter, where the optical background is clearly weakened and more CSs have emerged. The characteristic in Fig. 2, taken with a comb filter, shows an extended region at lower current where there is coexistence of the CS and a background-free state (the non-lasing off-state of the VCSEL).

Further evidence for motility of CSs is shown by moving the comb filter vertically (see the other panels in Fig. 4). The CSs react by a change of position. Within some areas of the sample, their shift is quasi-continuous, in others they seem to ‘jump’ from one preferred location to the other. Their motility distinguishes CS from fundamental modes of bistable small-area laser defined, e.g., by micro-machining. Its utilization enables new features as all-optical delay lines, optically controlled beam steering and self-alignment to different kinds of external inputs.

The experiments shown in Fig. 4 reveal also (as do the images in Fig. 3) that the CS do not have complete freedom of location in the present device, but tend to be attracted to, and trapped by, certain ‘defects’. Trapping effects were also found in other CS systems based on similar VCSELs [11, 15]. These defects are no doubt due to local inhomogeneities in the active layer (temperature or carrier density inhomogeneities) and/or the mirror layers (index inhomogeneities). The sensitivity of the CS location to such imperfections suggests a diagnostic application, i.e. that operation of a VCSEL in CSL mode can reveal structural defects not amenable to conventional microscopy techniques.

There is a novel and interesting self-induced force acting on the CS in our system. The GHz spread of CS frequencies means the emission frequency cannot be locked to the grating’s peak feedback frequency (see also [17]). Any detuned beam is fed back at a slightly different angle from its emission, which induces a phase gradient (of $2.9\ \text{mrad}/\mu\text{m}/\text{GHz}$) across the CS. Phase gradients are

well known from other CS systems to exert forces, leading to CS drift in an otherwise homogeneous system [23]. This means that the preferred CS locations in our system are actually equilibria between attracting defect forces and grating-induced tilt forces. We have confirmed the presence of a significant tilt-force by reversing the orientation of the grating, which leads to small shifts in all the preferred CS locations. The directions of these shifts are consistent with the tilt-force model, and their signs indicate that all the CS are blue-detuned from the grating peak, i.e. between the grating and VCSEL frequencies.

We observe a scatter, in the range of few mrad, in the centers of the far-field intensity distributions of different CS, consistent with equilibrium between defect and tilt forces being attained with tilts of a few mrad. This tilt is much smaller than the angular acceptance of the VCSEL resonance (see above), and so the effect on feedback efficiency is small. Direct experimental measurement of the tilt is quite difficult, however, because it seems to be much smaller than the angular far-field width of a CS, typically 44 mrad.

The switching behavior shown in Fig. 3 is also consistent with the defect model including the grating-induced force. Switch-on works well with the WB directly on the target location. For switch-off the WB is positioned to the side, so as to perturb the trap and initiate erasure, probably via carrier effects. However switch-off is not possible for every orientation of the WB with respect to the CS. When the phase gradient is oriented so as to direct the CS towards the trap, the CS reappears after the WB is removed. At these orientations switch-on is possible, however. Reversing the grating, and thus reversing the direction of the phase gradient, swaps these locations to the other side of the CS.

The switching sequence shown in Fig. 3 was performed with quasi-cw beams (i.e. by mechanically opening and closing the beam path of the WB for some seconds) because in that case the injection is easily visualized. How-

ever, switch-on and switch-off are also possible with a pulsed WB. The minimum pulse length investigated is 25 ns, with switch delays in the 10 ns range, and is limited by the available acousto-optic modulator [24]. Polarization and frequency-detuning between CS and WB are not critical but will influence the necessary switching energy and the resulting time delay. Switching off with a pulse aimed directly on the CS location is also possible, and works reliably.

In conclusion, we have demonstrated cavity-soliton microlasers in a semiconductor-based system and their all-optical control. The control is incoherent, i.e., there are no stringent phase or frequency requirements on the external beams used for writing, erasing or manipulation of the CS. This makes the scheme robust for applications. We anticipate that switching times are limited both by the external cavity round-trip time and by carrier relaxation. The latter could be improved by engineering of the carrier lifetime [25, 26]. With regard to round-trip time, we have preliminary evidence of CS in a short cavity closed by a volume Bragg grating [27]. Thus there is every prospect that use of microoptics (potentially to the level of monolithic integration) will allow significant improvements in both speed and compactness of these devices.

Acknowledgements

This work was supported by the European Union within the FunFACS project and by the Faculty of Science of the University of Strathclyde with a starter grant. We are grateful to FunFACS partners and to P. Paulau, N. A. Loiko, and A. V. Naumenko for many useful discussions and suggestions. M. Sondermann and F. Marino contributed to preliminary experimental stages of this work, discussions with J. R. Tredicce stipulated it.

-
- [1] N. Akhmediev and A. Ankiewicz, eds., *Dissipative solitons*, vol. 661 of *Lecture Notes in Physics* (Springer, New York, 2005).
 - [2] D. Cotter, R. J. Manning, K. J. Blow, A. D. Ellis, A. E. Kelly, D. Nesses, I. D. Philips, A. J. Poustie, and D. C. Rogers, *Science* **286**, 1523 (1999).
 - [3] V. Y. Bazhenov, V. B. Taranenko, and M. V. Vasnetsov, *Proc. SPIE* **1840**, 183 (1992).
 - [4] M. Saffman, D. Montgomery, and D. Z. Anderson, *Opt. Lett.* **19**, 518 (1994).
 - [5] V. B. Taranenko, K. Staliunas, and C. O. Weiss, *Phys. Rev. A* **56**, 1582 (1997).
 - [6] N. N. Rosanov, *Spatial hysteresis and optical patterns*, Springer Series in Synergetics (Springer, Berlin, 2002).
 - [7] M. Bache, F. Prati, G. Tissoni, R. Kheradmand, L. A. Lugiato, I. Protchenko, and M. Brambilla, *Appl. Phys. B* **81**, 913 (2005).
 - [8] N. N. Rosanov, S. V. Fedorov, and A. N. Shatsev, *Phys. Rev. Lett.* **95**, 053903 (2005).
 - [9] G. I. Stegeman and M. Segev, *Science* **286**, 1518 (1999).
 - [10] L. A. Lugiato, *IEEE J. Quantum Electron.* **39**, 193 (2003).
 - [11] S. Barland, J. R. Tredicce, M. Brambilla, L. A. Lugiato, S. Balle, M. Giudici, T. Maggipinto, L. Spinelli, G. Tissoni, T. Knödel, et al., *Nature* **419**, 699 (2002).
 - [12] V. B. Taranenko and C. O. Weiss, *Appl. Phys. B* **72**, 893 (2001).
 - [13] S. Barbay, Y. Ménesguen, X. Hachair, L. Leroy, I. Sagnes, and R. Kuszelewicz, *Opt. Lett.* **31**, 1504 (2006).
 - [14] Y. Larionova and C. Weiss, *Opt. Exp.* **13**, 10711 (2005).
 - [15] X. Hachair, F. Pedaci, E. Caboche, S. Barland, M. Giudici, J. R. Tredicce, F. Prati, G. Tissoni, R. Kheradmand, L. A. Lugiato, et al., *IEEE J. Sel. Top. Quantum Electron.* **12**, 339 (2006).
 - [16] X. Hachair, L. Furfaro, J. Javaloyes, M. Giudici, S. Balle, J. Tredicce, G. Tissoni, L. A. Lugiato, M. Brambilla, and

- T. Maggipinto, Phys. Rev. A **72**, 013815 (2005).
- [17] A. Naumenko, N. A. Loiko, M. Sondermann, K. F. Jentsch, and T. Ackemann, Opt. Commun. **259**, 823 (2006).
 - [18] Y. Tanguy, T. Ackemann, and R. Jäger, Phys. Rev. A **74**, 053824 (2006).
 - [19] C. H. Henry, IEEE J. Quantum Electron. **18**, 259 (1982).
 - [20] P. Paulau, A. Scroggie, A. Naumenko, T. Ackemann, N. Loiko, and W. Firth, Phys. Rev. E **75**, 056208 (2007).
 - [21] M. Grabherr, M. Miller, R. Jäger, R. Michalzik, U. Martin, H. J. Unold, and K. J. Ebeling, IEEE J. Sel. Top. Quantum Electron. **5**, 495 (1999).
 - [22] O. E. Martinez, IEEE J. Quantum Electron. **24**, 2530 (1988).
 - [23] W. J. Firth and A. J. Scroggie, Phys. Rev. Lett. **76**, 1623 (1996).
 - [24] Y. Tanguy, T. Ackemann, and R. Jäger, subm. to Opt. Exp. (2007).
 - [25] A. Garnache, S. Hoogland, A. C. Tropper, I. Sagnes, G. Saint-Girons, and J. S. Roberts, Appl. Phys. Lett. **80**, 3892 (2002).
 - [26] E. A. Avrutin, J. H. Marsh, and E. L. Portnoi, IEE Proc.-Optoelectron. **147**, 251 (2000).
 - [27] N. Radwell, Y. Tanguy, and T. Ackemann (2007), unpublished.